

Full-waveform seismic inversion at reservoir depths

T Nangoo, M Warner, J Morgan, A Umpleby, I Stekl (Imperial College London)
and A Bertrand (ConocoPhillips)

Overview

3D full-waveform inversion (FWI) has been most effective when it has been applied to long-offset, post-critical, refracted seismic arrivals to recover a high-resolution macro velocity model within relatively shallow heterogeneous overburden. Subsequent depth migration of deeper short-offset, sub-critical, reflected arrivals using the resultant shallow velocity model significantly improves reflection imaging. In such applications, the FWI velocity model is typically accurate to depths of no more than 1 to 2 km; see Sirgue *et al* (2009) for isotropic, and Ratcliffe *et al* (2011) for anisotropic, examples from the North Sea. However, the full promise of FWI techniques will only be realised when they are applied directly at reservoir depths to recover physical properties within the reservoir sequence. In this paper, we apply 3D anisotropic acoustic full-waveform tomographic inversion to a North Sea wide-angle OBC dataset, and demonstrate that our recovered velocity model is indeed realistic within the chalk reservoir sequence to depths of 4000 m. We achieve this by careful parameter selection, and especially by appropriate spatial preconditioning of the velocity update at each iteration. Because we use predominantly wide-angle refracted arrivals in the inversion, we are able to undershoot and image within the otherwise seismic obscured area beneath a shallow gas cloud that overlies the reservoir.

Methodology and Data

The OBC multi-component dataset that we have used is located in the Norwegian North Sea in the Ekofisk area, where intercalated clastics overlie an anticlinal chalk reservoir sequence that lies between 3 and 4 km depth. The presence of gas in the overburden silt and sandstone acts as a major challenge to conventional seismic imaging within and around the chalk reservoir. Previous work on the nearby Valhall field (Sirgue *et al*, 2009) and in the Tommeliten study area (Ratcliffe *et al*, 2011) has shown significant improvements in near-surface velocity structure using full-waveform inversion techniques, and consequently in the subsequent depth migration of the deeper reservoir structure.

The 3D dataset consists of three swaths of eight cables each, acquired with a staggered orthogonal geometry in flip-flop mode. This study used a subset of the hydrophone data only. Shot-receiver reciprocity was applied, the data were sub-sampled in space, and a total of 30,000 original shots and 1440 receivers were retained. The subset had sources with 75 m spacing in-line and cross-line, and receivers with 100 m in-line and 300 m cross-line spacing. The maximum offset is around 11 km, and there is full azimuthal coverage. The inversion is implemented in 3D using a methodology similar to that described by Warner *et al* (2010). An acoustic finite-difference algorithm is used with a multi-scale approach in the time domain that honours TTI anisotropy which can be up to 20% in these data.

Our FWI technique is driven principally by wide-angle refracted diving waves, in the frequency range 3-7 Hz. Pre-processing of the raw hydrophone data consisted only of low-pass filter and inside/bottom mute to remove deeper reflections, guided waves and converted shear waves. At far offsets, wide-angle and post-critical reflections from the chalk are recorded at the same time as the transmitted energy, and these reflections are included in the inversion. Surface multiples, and source and receiver ghosts are retained within the data, and these are modelled correctly during FWI. The data were trace-equalised during FWI so that the inversion fits relative amplitudes within a single trace, but not between traces. We invert a different subset of only 120 point sources at each iteration; we find that this strategy is much more effective than iterating every source at every iteration.

In any practical 3D FWI scheme, there are a large number of parameters that can be fine tuned to optimise the inversion for particular problems – we have optimised those parameters using extensive synthetic testing and repeated inversion of the field data. The recovered FWI model was assessed against filtered sonic velocities using a depth-varying, zero-phase, high-cut filter, to obtain the same spatial variation in velocity that is recoverable using FWI. The results were validated by comparing: (1) filtered sonic logs from four wells with the FWI velocities, (2) the geometry of the recovered FWI velocity model with the geometry of PSDM reflectors, (3) initial and final modelled with field seismic data at low frequencies, (4) 3D PSDM results using initial and final models, and by (5) checkerboard-perturbation recovery at reservoir depths using the final FWI model.

Results

At depths of 3-4 km, the final inversion recovered an asymmetric anticline consisting of laterally continuous, inter-bedded layers of relatively low and high velocity (Figures 1 and 2). This complex velocity-depth relationship, which is typical of carbonate rocks, was recovered from a starting model with a simple velocity gradient. Carbonates show little direct correlation between acoustic properties and age or burial depth, and velocity inversions with increasing depth, such as obtained in our recovered model, are common. Reflectors in an original PSDM reflection image correlate accurately with the recovered layering in the FWI velocity model; these were derived from entirely independent datasets: the former from sub-critical reflections, the latter from wide-angle arrivals.

At the crest of the chalk anticline, directly below a gas cloud in the overburden rocks, a distinct low-velocity anomaly is recovered in the reservoir chalks, Figures 1(b) and 3. Depth slices at 3250 m, through the recovered model, Figure 3, highlight this feature, which was not present in the starting model but which is indicated in the well logs, Figure 1(j). It is significant that this anomaly is imaged entirely using transmitted arrivals that undershoot the gas cloud in the overburden; these arrivals reveal a region that is otherwise obscured in the PSDM volume, Figure 1(d), because of scattering of reflected energy within the overlying gas cloud.

Although the inversions proceeded without prior knowledge of the well data, the vertical velocities recovered by FWI at the well positions, both beneath and to the side of the gas cloud, better follow the trends in the sonic velocities from the wells than does the starting model which was obtained using anisotropic reflection tomography and well ties, Figure 1(j). The match between the wells and the FWI data are not exact. The resolution of FWI is around half the shortest local seismic wavelength; in the gas cloud the resolution is about 120m, and in the chalk it is about 320m. We do not invert for anisotropy during the FWI which is likely to be anomalous within the gas cloud, and we assume a single relationship between density and velocity which is unlikely to represent accurately the properties of either the gas cloud or the chalk. Consequently we do not expect an exact match between FWI and well velocities, and are encouraged by the agreement in both trend and structure – in all cases the FWI results move from the starting model towards the sonic velocities.

Typically offsets of three to six times the target depth are needed to obtain the wide-angle transmitted arrivals that FWI requires to update the macro-velocity model (Warner *et al*, 2010). However, at long-offset and low-frequency, the Fresnel zones are large so that full-waveform data are sensitive to deeper parts of the model which may not at first sight appear accessible. Synthetic checkerboard tests demonstrate that, with our acquisition geometry (offsets to 11 km), sufficient wide-angle data are present to obtain useful updates down to about 4 km depth (Figure 4). Large macro-scale checkerboard patterns are clearly recovered at such depths, while the recovery of the smaller checkerboard varies spatially, with some small checkers clearly imaged and others less well resolved. These tests increase our confidence in the recovered velocity model across the reservoir chalks.

Conclusion

Full-waveform tomographic inversion at low frequencies was able to obtain a high-resolution velocity model at reservoir depths to 4 km, below a complex overburden of channels and gas-charged layers. The recovered structure is in agreement with sonic velocities from wells that penetrate to reservoir depths, and with an independent migrated volume. The key ingredient that allowed this was careful and extensive parameter testing prior to final inversion; we are working towards automating this step.

- Ratcliffe, A., Win, C., Vinje, V., Conroy, G., Warner, M., Umpleby, A., Stekl, I., Nangoo, T. & Bertrand, A. [2011] FWI: A North Sea OBS case study. SEG Expanded Abstracts 30, pp 2384.
- Sirgue, L., Barkved, O.I., Van Gestel, J.P., Askim, O.J. & Kommedal, J.H. [2009] 3D waveform inversion on Valhall wide-azimuth OBC. 71st EAGE Conference, Extended Abstracts, U038.
- Warner, M., Umpleby, A., Stekl, I. & Morgan, J. [2010] 3D full-wavefield tomography: imaging beneath heterogeneous overburden. 72nd EAGE Conference, Workshop, WS6.

Acknowledgements

We thank the PL044 partnership: ConocoPhillips Skandinavia AS, Total E&P Norge AS, ENI Norge AS, Statoil Petroleum AS for their permission to use their data and publish this work which was sponsored by the Fullwave III consortium. We also gratefully acknowledge support and advice throughout the project from Andrew Ratcliffe, Vetle Vinje and Graham Conroy of CGGVeritas.

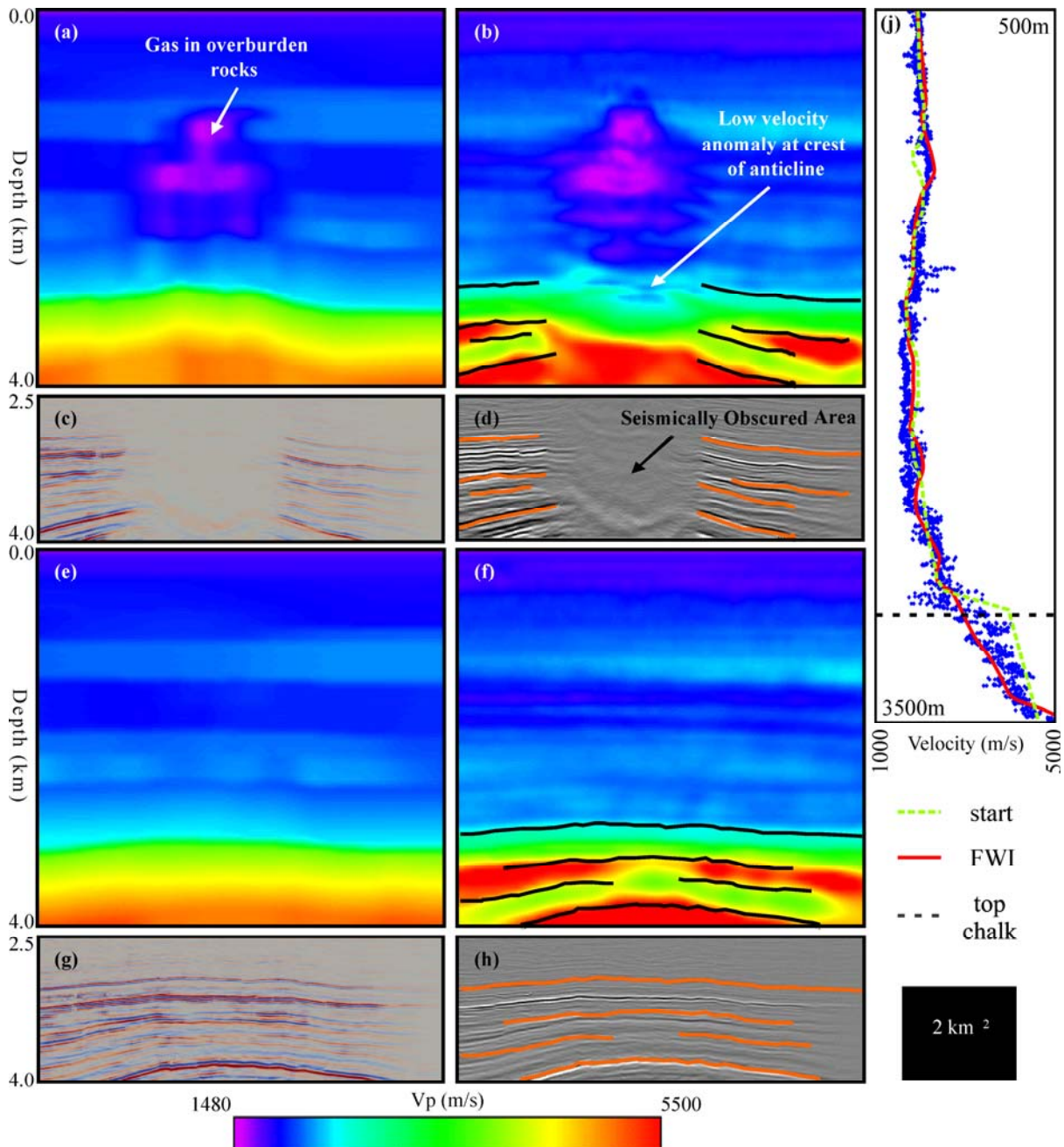


Figure 1 Vertical slices through: (a) & (e) starting model; (b) & (f) recovered FWI velocity model; (c) & (g) PSDM volume independent of FWI without interpretation; (d) & (h) interpreted PSDM with the bright reflectors highlighted. (a – d) show slices through the overlying gas cloud, while (e – h) are corresponding slices away from the gas cloud. (b) and (f) show that the recovered velocity layering correlates well with reflectors in the PSDM. (j) shows one of the well ties: blue dots are measured sonic velocities, green dashed curve shows vertical velocity from the starting model, red curve shows the FWI-recovered vertical velocity averaged over half a wavelength around the well position. This well penetrates both the gas cloud and the low-velocity anomaly at the crest of the anticline though it is offset from the centre of both of these features.

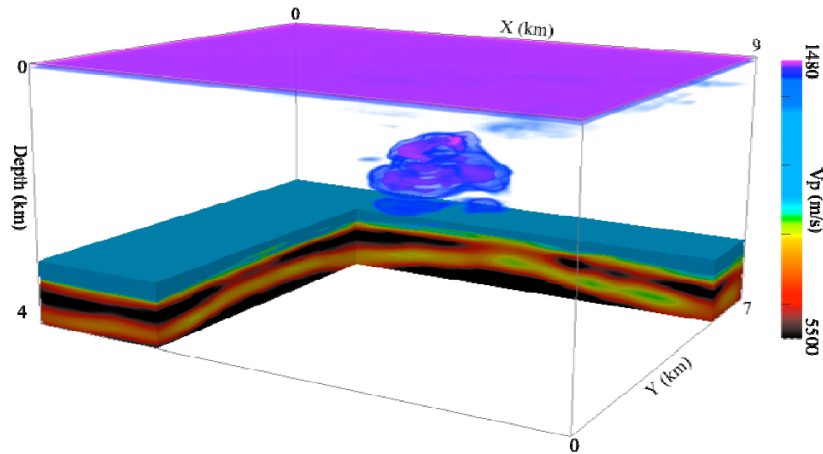


Figure 2 3D cube (4km deep) through the recovered FWI velocity model showing the lateral continuity of the reservoir chinks beneath the gas cloud in the overburden.

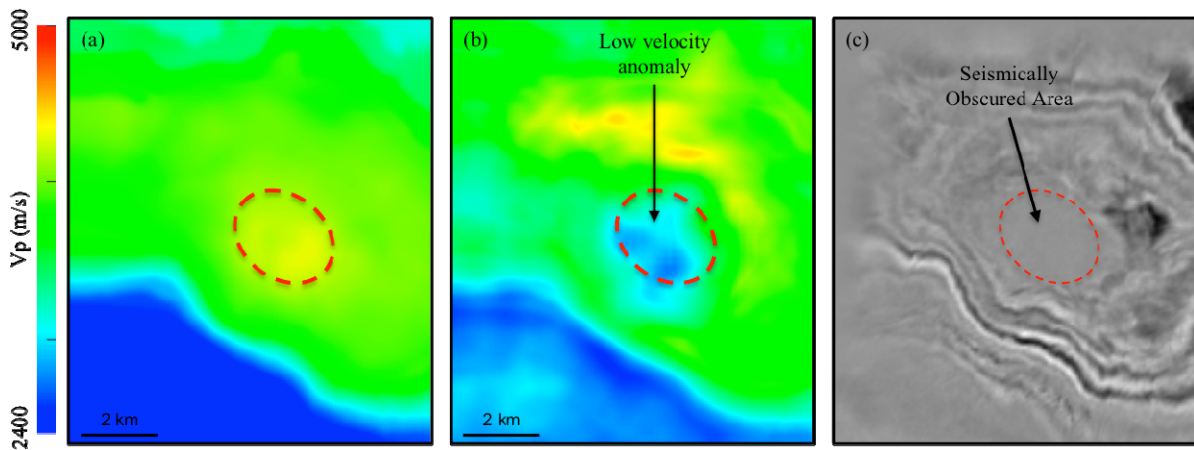


Figure 3 Depth slices at 3250 m through the (a) starting, (b) final recovered velocity models, and (c) original PSDM volume prior to FWI inversion. The dashed red circles highlight the area that is seismically obscured in the migrated reflection volume. In contrast, FWI undershoots the obstruction.

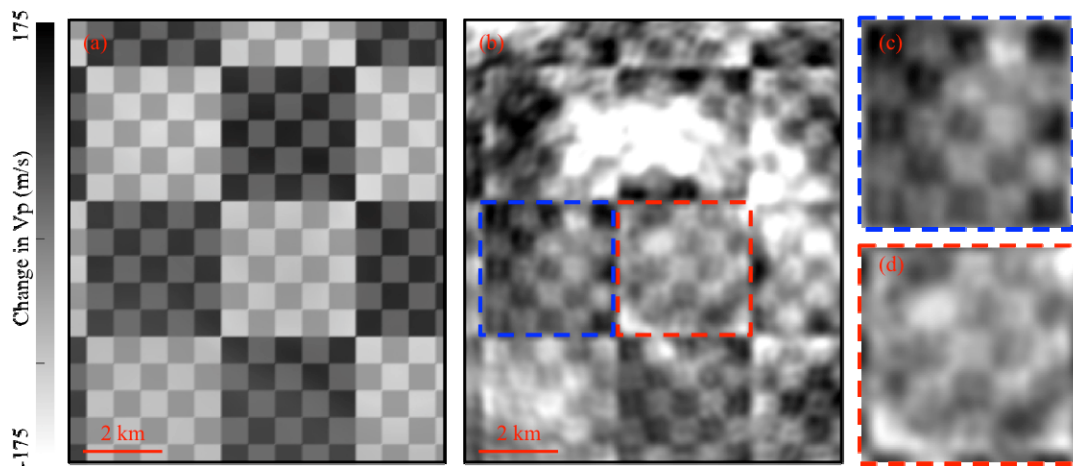


Figure 4 Depth slices at 3250m to recover a chequerboard perturbation to the final FWI model. (a) true velocity perturbation, (b) recovered perturbation, the dashed red square highlights the seismically obscured area using reflection techniques. (c) and (d) are zoomed images from (b).